X-615-69-77
PREPRINT

NASA TM X-63484

A REVIEW OF THE THEORIES CONCERNING THE EQUATORIAL F2 REGION IONOSPHERE

RICHARD A. GOLDBERG

MARCH 1969

GSFC
GODDARD SPACE FLIGHT CENTER
GREENBELT, MARYLAND
TO BE PUBLISHED IN PROCEEDINGS OF THE IEEE

A REVIEW OF THE THEORIES CONCERNING THE EQUATORIAL F2 REGION IONOSPHERE

by

Richard A. Goldberg

March 1969

NASA-Goddard Space Flight Center
Greenbelt, Maryland 20771

PRECEDING PAGE BLANK NOT FILMED

CONTENTS

ABSTRACT

The most characteristic feature of the equatorial F region ionosphere is the equatorial geomagnetic anomaly. This phenomenon has been known for nearly thirty years from bottomside measurements, but only recently have topside Alouette data provided the overall description to enable the development of theoretical models. It appears that the major contribution to this effect lies in the interaction of the ionosphere with the earth's magnetic field via mechanisms causing drifts and currents. However, other theories have considered control due principally to production, loss and temperature effects. This paper reviews relevant theoretical analyses and compares the theoretical predictions with data available from the Alouette I topside sounder.

INTRODUCTION

In recent years, the equatorial F-region of the ionosphere has received a great deal of attention because of its rather special electron density distributions. Of major interest is the daytime variation of electron density with latitude, often referred to as the geomagnetic anomaly.

Whereas the midlatitude F-region is nearly horizontally stratified with latitude, the equatorial F-region exhibits variations that indicate a strong interaction of the ionospheric plasma with the earth's magnetic field. Ground-based ionosondes have provided a wealth of information concerning this behavior in the bottomside F-region for nearly thirty years. However, little was known concerning the topside until studies were made by analysis of data from the Alouette topside sounders. Another paper in this issue (King) discusses the morphology of the topside equatorial ionosphere. This paper is concerned with a review of theoretical studies directly related to the phenomena described by King.

The theories covered by this review are in two main groups. The first group attempts to explain the observed phenomena by seeking specific causal mechanisms. Such studies have investigated the possible contributions of electron diffusion, electrodynamic drift caused by electric fields propagating from E-region altitudes, ion drag, neutral winds, electron production and loss, temperature variations, and photoelectron effects. These model studies nearly all require complex computer solutions of the steady state continuity equation for electrons and produce results in varying degrees of agreement with the observed morphology.

A second group of studies treats the problem semiphenomenologically. The distribution of electron density along some boundary crossing magnetic field lines is thought of as an implicit function of most conceivable causes, such as production, loss, drifts, temperature, etc. This boundary condition is then used as a known input to the problem of diffusion along field lines under the influence of gravity in a region where interactions of the plasma with the neutral atmosphere are small, leading to an analytic technique for describing the topside electron density distribution both qualitatively and quantitatively. This approach provides a simple method for learning how variations in ion composition and temperatures can alter the distribution or conversely, what these parameters are from the distribution.

Mention is also made of recent studies of the diurnal behavior of the effects under consideration. Such studies involve solution of the time dependent continuity equation and are limited because of the complex procedures required.

GENERAL PROPERTIES OF THE EQUATORIAL F2 REGION

This section reviews the prominent features associated with the equatorial F-region ionosphere (geomagnetic anomaly). Figure 1 shows the average noontime equinoctial bottomside electron density distribution. The upper part of Fig. 2 is representative of the extension of these curves into the topside F region at east longitude regions near Singapore. We note that Lockwood and Nelms (1964) have observed a less pronounced geomagnetic anomaly in regions about the 75th west meridian, indicating a longitudinal variation in the equatorial distribution. Goldberg (1966) has offered an explanation of such effects based upon differences in magnetic declination between the two geographic regions. However, longitudinal effects are not sufficiently well documented to be fully accounted for at the present time.

Neglecting deviations due to longitude, the main features are:

1. The constant height electron density profiles and the peak electron density profile (NmF2) exhibit a minimum (trough) at the magnetic equator with maxima (crests) on either side. For NmF2, the crests occur at approximately $\pm 30°$ dip.

2. Figure 2 illustrates the alignment of the crests with a specific magnetic field line. As seen in Fig. 1, this field line dependence gradually decreases with decreasing altitude and hence, increasing plasma-neutral collisions. Others have found (e.g. Thomas, L., 1968) that the greatest symmetry with respect to magnetic dip occurs when the noontime subsolar point lies on the dip equator (dip equinox).

3. As indicated in Fig. 3 and also observed by Thomas, J. O., (1962), the height of the F2 peak (h_mF2) is greatly boosted at the magnetic equator.

4. During solstice seasons, the crests in the summer hemisphere are broader and lower than those in the winter hemisphere (Thomas, L., 1968; Fitzenreiter, Goldberg, and Krishnamurthy, 1967). h_mF2 is also distorted with the higher side of the peak in the summer hemisphere.

5. The anomaly forms between 9:00 and 11:00 LMT and normally is maintained until approximately 22:00 LMT (Lockwood & Nelms, 1964; Fitzenreiter, Goldberg, and Krishnamurthy, 1967). Later, the anomaly converts into a single crest at the equator, followed in the early morning hours by nearly horizontal stratification with latitude.

6. The above properties refer only to quiet day conditions. The behavior of the anomaly during storm conditions is not clear. During some storms, the trough appears to fill in (enhancement) causing a less pronounced anomaly distribution (King, et. al., 1967). Others, (Dunford, 1967) find the opposite trend for disturbed conditions. Sato (1968) has categorized storms as D type or N type depending on whether enhancement or depletion is observed, and finds that most D type effects occur or begin during daylight hours.

7. The equatorial ionosphere does not exhibit the above properties at altitudes approaching 1000 km. Chandra and Rangaswamy (1967) have shown that the distribution in this region can be described by an expression containing both solar and magnetic effects. However, no specific theoretical model has been presented and hence, no further mention of this region will be made in this paper.

CURRENT THEORIES

A. Causal Approach (Postulated Specific Mechanisms)

The first suggestion for explaining these equatorial features was offered by S. K. Mitra (1946). He proposed that electrons produced by solar ionization near the equator would diffuse along magnetic field lines causing enhancement of ionization in the vicinity of the anomaly crests. However, low electron production rates in the upper F-region led Martyn (1955), Maeda, K. (1955), and Hirono & Maeda, H. (1955) to speculate that the origin of such particles might arise from electrodynamic lifting near the equator rather than from direct solar ionization. This fountain effect (shown in Fig. 4 for midday) was discussed quantitatively by Duncan (1960) and the necessary diffusion rates were found to be reasonable. Spreiter & Briggs (1961) found that E-region electric fields could propagate to F-region levels allowing the required electrodynamic drifts to be generated, and H. Maeda (1963) derived the magnitude of F-region electric fields and the corresponding drifts. This concept has been the predominant mechanism postulated for the cause of the geomagnetic anomaly.

This approach begins with the continuity equation for electrons,

$$\nabla \cdot N\vec{v} = Q - L \tag{1}$$

Here N is electron density, $\vec{v}$ is the total electron velocity caused by diffusion and drifts, Q is electron production and L is electron loss. Geomagnetic control enters this equation through the velocity term. For convenience, let

$$\vec{v} = \vec{v}_{\parallel} + \vec{v}_{\perp} \tag{2}$$

where the subscripts refer to directions along or perpendicular to a magnetic field line. The expression for $\vec{v}_{\parallel}$ is dominated by diffusion under the influence of gravity and can be written as

$$\vec{v}_{\parallel} = -D\left[\sin I\left(\frac{1}{N}\frac{\partial N}{\partial r} + \frac{1}{2H_i}\right) + \frac{\cos I}{Nr}\frac{\partial N}{\partial \theta}\right] \tag{3}$$

where D, the diffusion coefficient, is dependent on ion and electron temperatures, collision frequencies between electrons, ions, and neutral particles, and ion and electron masses; I is the magnetic dip angle; H_i is the scale height of the ionized constituent; r and θ are polar coordinates in the meridian plane of the magnetic field. Equation (3) arises from the momentum transfer equations for electrons, ions, and neutrals neglecting the effects of viscous, Coriolis, tidal, and centrifugal forces. The approximations leading to this result for low latitudes can be found in Kendall (1962), Goldberg & Schmerling (1963), Chandra (1963), Chandra and Goldberg (1964). The last term on the right is the contribution from horizontal electron density gradients and is normally neglected for midlatitude diffusion and drift studies (cf. Ferraro, 1945 , for the first derivation of the midlatitude equation and Rishbeth, 1967a , 1968 for a more complete review of this subject).

The expression for $\vec{v}_{||}$ given by (3) is now substituted into (1) to provide a general equation for solution (Kendall, 1962; Goldberg & Schmerling, 1963). Modifications due to electromagnetic drifts are then added by including a term for $\vec{v}_{\perp}$. Diffusive forces are negligible compared to other forces contributing to $\vec{v}_{\perp}$. Finally, ion drag and neutral wind drifts are included as modifications to $\vec{v}_{||}$. In all cases discussed, thermal equilibrium and isothermal conditions are assumed.

The general equation for diffusion with or without drifts is next solved numerically. The parameters of this problem are adjusted until the equatorial vertical density profile produced is similar to that observed.

The first papers to use this approach (Kendall, 1963; Rishbeth, Lyon, and Peart, 1963), neglected the effects of $\vec{v}_{\perp}$ and considered diffusion with production and loss as the major physical processes. Their results produced a distribution exhibiting the properties of the geomagnetic anomaly qualitatively but on a much smaller scale than observed. Bramley & Peart (1964) next introduced a vertical drift near the equator by postulating the existence of an electric field in the westward direction, perpendicular to the magnetic meridian plane. In their first analysis, this drift was included as a perturbation effect and the results indicated that such an effect would produce an anomaly larger in scale than that obtained from diffusion alone.

Next, Moffett & Hanson (1965), Hanson & Moffett (1966), and Bramley & Peart (1965) independently developed numerical techniques for solving the continuity equation with electrodynamic drifts included as major effects. Both groups arrived at similar conclusions, that the earlier perturbation analysis of Bramley & Peart (1964) had led to valid results and that an upward drift of only a few meters per second was sufficient to generate most of the general properties of the distribution, both qualitatively and quantitatively. Figure 4 illustrates the electron fluxes associated with this model and vividly demonstrates the fountain effect. Figure 5 shows a typical set of electron density contours for an upward drift of 20.5 m/s. We note that this method typically produces much too small a variation in $h_m F2$ with latitude.

Concurrently, the effect of ion drag on the geomagnetic anomaly was also being considered. In this process ion movements set the neutral atmosphere into horizontal motion via collisions. This neutral wind then produces an additional component of ion velocity along the magnetic field lines. This process was considered because, as pointed out by Kendall and Windle (1965a), F-region drift speeds of 20 m/s predicted from dynamo theory (H. Maeda, 1963) were much larger than those required to account for the geomagnetic anomaly. Moreover, midlatitude theories (e.g. Dougherty 1961) indicated that ion drag would reduce the magnitude of electrodynamic lifting.

Chandra and Goldberg (1964) first discussed a technique for calculating the effects of ion drag on the neutral atmosphere in the equatorial region and suggested that such effects mig' be observable as magnetic control of the neutral atmosphere in the lower F-region. Kendall and Windle (1965b) studied this effect by including it in the continuity equation for diffusion alone. They found that when the horizontal ion and neutral velocities are equal, the ion drag process can produce the observed depth of the anomaly trough but cannot quantitatively account for the latitudinal width between crests. Windle and Kendall (1965) investigated the effects of assuming the horizontal neutral velocity to be a fixed proportion (less than 1) of the horizontal ion velocity and found that the two velocities must be nearly equal before the required depth of the trough can be produced.

The asymmetry of the anomaly associated with solstice conditions has also been examined using the causal approach. Most analyses assume that a horizontal neutral wind blows across the equator. Varnasavang, Hargreaves and Kendall (1965), Hanson and Moffett (1966), Bramley and Young (1967), and Rishbeth (1967b) all conclude that a higher electron density crest will appear in that hemisphere from which the wind is blowing. To agree with observation, the wind must blow from the summer to winter hemisphere. Figure 6 shows the theoretical asymmetry produced by a horizontal wind of 60 m/s and a vertical upward drift of 15 m/s. The observed asymmetry is more pronounced than illustrated here, indicating either the existence of stronger transequatorial winds or the possibility of other contributing mechanisms.

B. Semiphenomenological Approach

Most of the studies discussed in the previous section have concluded that processes such as electrodynamic drift, neutral winds, and ion drag will have a relatively small effect on the distributions in the topside equatorial F-region. Furthermore, Kendall and Windle (1965b) have shown that the topside region between the anomaly crests would not be subject to ion drag effects and Baxter, Kendall, and Windle (1965) have shown that the topside distribution must be supported by production and loss effects from below. These results indicate that the topside distribution could be controlled primarily by diffusive equilibrium modified by the effects of production, loss, and drift from below. Using this concept, a semiphenomenological theory has also been developed. This approach does not postulate specific mechanisms for the basic causes of the geomagnetic anomaly. Instead, it accepts the vertical density profile at the magnetic equator or some other density profile crossing magnetic field lines as an observed boundary condition, and then proceeds to calculate the electron density at other latitudes and altitudes.

In this approach, plasma-neutral collisions are neglected in the momentum transfer steady state equations. As in the causal approach, viscous effects, Coriolis, tidal, and centrifugal forces are also considered unimportant in the region of study. The major effects considered are pressure gradients, gravity, electric fields and production and loss; the latter three via the assumed boundary condition. The assumptions lead to a relatively simple diffusive equilibrium-like equation for the electron density

$$\sin I \left(\frac{1}{N\tau} \frac{\partial N\tau}{\partial r} + \frac{1}{2H_\tau} \right) + \frac{\cos I}{N\tau r} \frac{\partial N\tau}{\partial \theta} = 0. \tag{4}$$

The solution of equation (4) along a magnetic field line is

$$N(r, \theta) = \frac{N(r_0)\, \tau(r_0)}{\tau(r, \theta)} \exp - \int_{r_0}^{r} \frac{dr}{2H_\tau} \tag{5}$$

where r is a geocentric radius, θ is colatitude, r_0 is usually the equatorial geocentric radius to the field line apex, τ is the average of the electron and ion temperatures, and H_τ is a modified scale height of the ionizable constituent. Normally, electron and ion temperatures are assumed equal and constant so that H_τ is identical to the scale height of the ionizable constituent (cf. Chandra and Goldberg, 1964 and Goldberg, 1965 for a complete discussion and derivation of the above equations).

Goldberg and Schmerling (1962) first used this technique to produce results showing agreement with data which improved with increasing altitude. This work employed a vertical topside profile of electron density at the equator, exponential in form and having a different scale height than that of the ionized constituent. An attempt was then made to solve the steady state continuity equation (1) analytically (Goldberg and Schmerling, 1963). A power series solution for electron density was obtained including explicit terms for production and loss, although these terms were neglected in the evaluation of the results. A Chapman-like boundary condition for the vertical electron density profile as the equator was substituted for the earlier exponential form. The results in this work predicted the gradual decay of the anomaly with altitude in the topside but showed poor agreement with bottomside measurements.

Goldberg, Kendall and Schmerling (1964) next demonstrated the equivalence of the two solutions (series and closed form) and applied the Chapman-like vertical boundary condition to equation (5). Comparison was made with Alouette 1 data of King by matching and estimating parameters leading to Fig. 2. As illustrated, both theory and measurements indicate that the crests move equatorward along a field line with increasing altitude.

In view of the fact that the observed vertical profile at the equator is only roughly Chapman-like in form, the above results were very encouraging. Next, Chandra and Goldberg (1964) attempted to fit the boundary with a more realistic vertical profile and obtained a substantial improvement. Finally, Baxter and Kendall (1965) numerically applied an actual boundary condition, as measured by Alouette 1 along a fixed height path, and obtained a nearly perfect fit with the additional data measured during the same satellite pass.

Workers have also employed this technique to calculate latitudinal variations of other ionospheric quantities. For example, Chan (1966) produced dip latitude variations in mean ionic mass, temperature, and scale height. Rishbeth, Van Zandt, and Norton (1966) applied this type of analysis to topside vertical electron density profiles and calculated field aligned profiles in good agreement with the measured results from Alouette 1. In addition, they deduced plasma temperature and ion composition values in good agreement with data from the Ariel 1 satellite.

This approach is much easier to use than the causal approach for the analytical study of effects caused by such mechanisms as vertical drifts and temperature variations. Baxter (1964) and Baxter, Kendall and Windle (1965) applied the power series solution technique of Goldberg and Schmerling (1963) to the continuity equation with the inclusion of electrodynamic drift. They obtained a closed form expression identical to that for diffusion alone except for an extra term due to drift. The effects of drift were then studied quite simply using the Chapman-like boundary condition at the equator. Similar conclusions to those of the causal approach were reached concerning the effects of such drifts, including the result that a vertical upward drift would greatly affect the bottomside but would modify the topside distribution only slightly. The results of Baxter, Kendall and Windle (1965) also indicate that bottomside production and loss processes are essential to provide a source of electrons to support the topside distribution.

The only study of thermally caused modifications to the geomagnetically controlled electron density distribution has been made by including the empirical variation of electron temperature with height in the terms $\partial N\tau/\partial r$ and H_τ of equation (5) (Goldberg, 1965). Starting with the model of Goldberg, Kendall, and Schmerling (1964), this study has shown that the inclusion of the effect of electron temperature variation with height provides a better fit with bottomside data. In addition, the model produces improved results to higher latitudes, especially for h_mF2 and NmF2 as illustrated in Fig. 3.

The semiphenomenological approach can also be used to deduce possible mechanisms for maintaining the topside distribution. Goldberg (1965) has calculated the amperian currents necessary to support the midday distribution if such a distribution is close to steady state. These currents flow to the east in the equatorial trough and to the west at latitudes beyond the crests. By extending the analysis to morning and evening, observed magnetic declination effects at such times can be accounted for by the existence of small currents flowing toward the equator in the morning and away from the equator in the evening (Goldberg, 1966). Such currents are also found to be sufficient for the support of the morning rise and evening decay in plasma pressure. The consistency of these results suggests an alternate mechanism for the cause of the anomaly, at least in the topside. Currents generated in the morning and evening by longitudinal plasma pressure gradients would have to form closed loops flowing counter clockwise in the northern hemisphere and clockwise in the southern hemisphere. The daytime anomaly distribution would then be caused by the east-west flow of these currents to attain closure, thereby perturbing the expected horizontally stratified distribution under the influence of diffusive equilibrium at midday to form the geomagnetic anomaly.

C. Time Dependent Solutions

Theoretical study of the time dependent topside equatorial ionosphere has been rather limited because of the great complexity introduced by this one additional variable. Hanson & Moffett (1966) used a transient analysis to study the variation of a distribution along a specific field line from an initial condition to a final stationary state. Their results indicate that steady state noontime observations could occur in a sufficiently short period (a few hours) for the steady state noontime analysis to be valid.

Varnasavang (1967) studied the nighttime equatorial F behavior by modifying the continuity equation (Kendall, 1962) for a region precisely at the equator and by neglecting electron production. With these simplifications, he was able to solve the time dependent continuity equation analytically, given an initial sunset condition. He found that an evening rise or lowering of h_mF2 would be related to an upward or downward electrodynamic drift, respectively.

More recently, Baxter and Kendall (1968) have discovered a technique for fully solving the time dependent continuity equation with electrodynamic effects included. Figure 7 is a global plot of NmF2 for an upward drift of 20 m/s from their analysis. The time of formation and decay of the anomaly roughly agrees with measurement and can be fit more accurately by adjustment of such parameters as drift. These results further indicate that electrodynamic drift is a significant mechanism contributing to the observed distribution of the equatorial F-region.

D. Other Theoretical Considerations

The theoretical evidence for electrodynamic lifting and ion drag as two major contributors to the geomagnetic anomaly make it unlikely that any other process could play a dominant role in creating this effect, at least below h_mF2. However, two additional factors have been proposed as possible mechanisms influencing the distribution, especially in the topside F-region where drift effects weaken. Mariani (1964) has suggested that photoelectrons produced in the upper F-region would have sufficient lifetime to diffuse along field lines to other regions. His calculations indicate that a minimum depletion of such particles would occur in the region of the anomaly crests, thereby enhancing the magnitude of such crests.

Norton and Van Zandt (1964) have solved the time dependent continuity equation numerically by neglecting the divergence term relating to transport. They find that photoionization and recombination combined with a temperature model, which increases in the morning and levels out in the afternoon, can produce most of the features of the daytime equatorial ionosphere as observed precisely at the equator. The photoionization rates used suggest that Mitra's (1946) hypothesis of equatorial photoionization followed by diffusion along field lines may be a significant contribution. Awojobi (1965, a, b) followed a similar approach with a slightly modified loss function and concluded that geomagnetic control is not necessary to account for the distribution of the anomaly. This latter conclusion is probably not valid, as pointed out by Ostrow and Stewart (1967) and other works listed herein. However, there is no question that temperature can play an important role in influencing the shape of the equatorial distributions and yet, no inclusion of this effect has been offered in any of the causal approach studies.

SUMMARY AND CONCLUSIONS

We have reviewed the major theories dealing with the equatorial F-region by categorizing them into two basic groups – causal and semiphenomenological. The causal theories have postulated electrodynamic lifting at the equator, caused by electrostatic fields propagating from the E-region, as the basic mechanism responsible for forming the equatorial distributions. Ion drag effects partially cancel the effects of electrodynamic drifts and produce results in better agreement with observation. Transequatorial neutral winds have been postulated and may possibly account for solstice asymmetries. Finally, time dependent solutions have supported the use of steady state analysis and also accounted for the rise and decay of the anomaly.

The above analyses have required complex numerical computer solutions of the continuity equation to determine the effects of specific physical modifications. An alternate semiphenomenological approach makes use of the measured electron density distribution along a specific boundary crossing field lines and enables the effects of temperature and composition variation, drifts, and other effects to be studied simply and analytically. This approach can also lead to a consistent argument concerning a possible basic mechanism to sustain the topside distribution, viz. longitudinal plasma pressure gradients. Both approaches find that diffusive equilibrium-like distributions exist in the topside, but that plasma-neutral collisions and hence drifts play an increasingly important role with decreasing altitude.

Factors which probably make lesser contributions include photoelectron enhancements and variable temperature effects caused by non-thermal equilibrium and thermal gradients with height and longitude (time). At this time, the temperature variations have not been included in the causal approach to determine the degree of their importance.

The mechanisms postulated in the electrodynamic drift theory are consistent in that they produce agreement between observation and theoretical results, but are lacking in experimental verification. Recent studies of the topside ionosphere under storm conditions (King et. al., 1967; Dunford, 1967; Sato, 1968) indicate a possible correlation of F-region behavior with E-region effects. In addition, Drobzhev (1968) has found a correlation of F-region vertical drifts with E-region magnetic fluctuations. More work of this nature, plus measurements of F-region electric fields at midday is required to establish whether or not the fountain effect is the dominant mechanism causing the features under study. The trans-equatorial neutral winds currently postulated as the basic cause of transhemispheric asymmetries during solstice conditions likewise require further investigation. Finally, as Burkhard (1966) has stated, theories should also be extendable into midlatitude regions, since many of the magnetically controlled effects reach into such regions.

REFERENCES

Awojobi, O. A., "On the Ionospheric F2 Region Equatorial Anomaly," J. Atmos. Terr. Phys., 27, 1309-1311, 1965.

Awojobi, O. A., "Recombination Coefficient and the Pre-Noon Maximum of Electron Density in Ionospheric F2 Region," J. Atmos. Terr. Phys., 28, 375-384, 1966.

Baxter, R. G., "On the Theoretical Effects of Electrodynamic Drift in the Equatorial F2 Layer," J. Atmos. Terr. Phys., 26, 711-720, 1964.

Baxter, R. G., and P. C. Kendall, "Diffusion Equilibrium of the Topside Electron Density in the F2 Region," J. Atmos. Terr. Phys., 27, 129-132, 1965.

Baxter, R. G., and P. C. Kendall, "A Theoretical Technique for Evaluating the Time-Dependent Effects of General Electrodynamic Drifts in the F2 Layer of the Ionosphere," Proc. Roy. Soc. Lond., A 304, 171-185, 1968.

Baxter, R. G., P. C. Kendall and D. W. Windle, "Power Series Solution of the F2 Layer Diffusion Equation, J. Atmos. Terr. Phys., 27, 1263-1273, 1965.

Bramley, E. N., and M. Peart, "Diffusion and Electromagnetic Drift in the Equatorial F2 Region," J. Geophys. Res., 69, 4609-4616, 1964.

Bramley, E. N., and M. Peart, Diffusion and Electromagnetic Drift in the Equatorial F2 Region, J. Atmos. Terr. Phys., 27, 1201-1211, 1965.

Bramley, E. N., and Margaret Young, "Winds and Electromagnetic Drifts in the Equatorial F2 Region," J. Atmos. Terr. Phys., 30, 99-111, 1968.

Burkhard, O. M., "Some Remarks on Papers Concerning the Geomagnetic Anomaly of the F2 Layer," J. Atmos. Terr. Phys., 28, 1129-1130, 1966.

Chan, K. L., "On the Topside Ionosphere Over the American Continents," Radio Science, 1, 1158-1162, 1966.

Chandra. S., "Plasma Diffusion in the Ionosphere," J. Atmos. Terr. Phys., 26, 113-122, 1964.

Chandra, S., and R. A. Goldberg, "Geomagnetic Control of Diffusion in the Upper Atmosphere," J. Geophys. Res. 69, 3187-3198, 1964.

Chandra, S., and S. Rangaswamy, "Geomagnetic and Solar Control of Ionization at 1000 km," J. Atmos. Terr. Phys., 29, 259-265, 1967.

Croom, S., A. Robbins and J. O. Thomas, Two Anomalies in the Behavior of the F2 Layer of the Ionosphere," Nature, 184, 2003, 1959.

Dougherty, J. P., "On the Influence of Horizontal Motion of the Neutral Air on the Diffusion Equation of the F Region," J. Atmos. Terr. Phys., 20, 167-176, 1961.

Drobzhev, V. I., "Geomagnetic Control of Ionization's Vertical Drift in the F Region of the Ionosphere," Geomag. i Aeronomiya, 8, 176-177, 1968.

Duncan, R. A., "The Equatorial F Region of the Ionosphere," J. Atmos. Terr. Phys., 18, 89-100, 1960.

Dunford, E., "The Relationship Between the Ionospheric Equatorial Anomaly and the E Region Current System," J. Atmos. Terr. Phys., 29, 1489-1498, 1967.

Ferraro, V. C. A., "Diffusion of Ions in the Ionosphere," Terrestrial Magn. and Atmos. Elect., 50, 215-222, 1945.

Fitzenreiter, R., R. A. Goldberg, and B. V. Krishnamurthy, "Magnetic Declination and Solar Control of the Topside Ionosphere," NASA Rept. X-615-67-21, February, 1967.

Goldberg, R. A., "The Effect of a Variable Electron Temperature on the Equatorial Electron Density Distribution in the Upper Ionosphere," J. Geophys. Res., 70, 655-666, 1965.

Goldberg, R. A., "Equatorial Geomagnetic Anomaly and Its Associated Current System," J. Geophys. Res., 70, 5417-5424, 1965.

Goldberg, R. A., "A Theoretical Model for the Magnetic Declination Effect in the Ionospheric F Region," Annales Geophys., 22, 588-598, 1966.

Goldberg, R. A., and E. R. Schmerling, "The Distribution of Electrons Near the Magnetic Equator," J. Geophys. Res., 67, 3813-3816, 1962.

Goldberg, R. A., and E. R. Schmerling, "The Effects of Diffusion on the Equilibrium Electron Density Distribution in the F Region Near the Magnetic Equator," J. Geophys. Res., 68, 1927-1936, 1963.

Goldberg, R. A., P. C. Kendall and E. R. Schmerling, "Geomagnetic Control of the Electron Density in the F Region of the Ionosphere," J. Geophys. Res., 69, 417-428, 1964.

Hanson, W. B., and R. J. Moffett, "Ionization Transport Effects in the Equatorial F Region," J. Geophys. Res., 71, 5559-5572, 1966.

Hirono, Motokazu and Hiroshi Maeda, "Geomagnetic Distortion of the F2 Region on the Geomagnetic Equator," J. Geophys. Res., 60, 241-255, 1955.

Kendall, P. C., "Geomagnetic Control of Diffusion in the F2 Region of the Ionosphere – I. The Form of the Diffusion Operator," J. Atmos. Terr. Phys., 24, 805-811, 1962.

Kendall, P. C., "Geomagnetic Control of the Diffusion in the F2 Region of the Ionosphere – II. Numerical Results," J. Atmos. Terr. Phys., 25, 87-91, 1963.

Kendall, P. C., and D. W. Windle, "The Appleton Anomaly," Nature, 207, 964-965, 1965a.

Kendall, P. C., and D. W. Windle, "A Possible Explanation of the Appleton Anomaly of the F2 Layer; Dougherty's Theory of Ion Drag," J. Atmos. Terr. Phys., 27, 795-802, 1965b.

King, J. W., K. C. Reed, E. O. Olatunji, A. J. Legg, "The Behavior of the Topside Ionosphere During Storm Conditions," J. Atmos. Terr. Phys., 29, 1355-1363, 1967.

Lockwood, G. E. K., and G. L. Nelms, "Topside Sounder Observations of the Equatorial Anomaly in the 75° W Longitude Zone," J. Atmos. Terr. Phys., 26, 569-580, 1964.

Maeda, H., "Worldwide Pattern of Ionization Drifts in the Ionospheric F Region as Deduced from Geomagnetic Variations," The Ionosphere published by Institute of Physics and the Physical Society, London, 1963, pp. 187-190.

Maeda, Ken-ichi, "Geomagnetic Distortion in the F2 Layer," Physics of the Ionosphere, Physical Society, London, 1955, pp. 245-253.

Mariani, F., "Pitch-Angle Distribution of the Photoelectrons and Origin of the Geomagnetic Anomaly," J. Geophys. Res., 69, 556-560, 1964.

Martyn, D. F., "Theory of Height and Ionization Density Changes at the Maximum of a Chapman-like Region, Taking Account of Ion Production, Decay, Diffusion, and Total Drift," Physics of the Ionosphere, published by Physical Society, London, 1955, pp. 254-259.

Mitra, S. K., "Geomagnetic Control of Region F2 of the Ionosphere," Nature, 158, 668-669, 1946.

Moffett, R. J., and W. B. Hanson, "Effect of Ionization Transport on the Equatorial F Region," Nature, 206, 705-706, 1965.

Norton, R. B., and T. E. VanZandt, "The Daytime Equatorial F Layer," J. Atmos. Terr. Phys., 26, 1047-1054, 1964.

Ostrow, S. M., and F. G. Stewart, "On the Ionospheric F2 Region Equatorial Anomaly and the Geomagnetic Field," J. Atmos. Terr. Phys., 29, 1005-1010, 1967.

Rishbeth, H., "A Review of Ionospheric F Region Theory," Proc. IEEE, 55, 16-35, 1967a.

Rishbeth, H., "Transequatorial Diffusion in the Topside Ionosphere," Planet. Space Sci., 15, 1261-1965, 1967b.

Rishbeth, H., "On Explaining the Behavior of the Ionospheric F Region," Reviews of Geophys., 6, 33-72, 1968.

Rishbeth, H., A. J. Lyon, and Margaret Peart, "Diffusion in the Equatorial F Layer," J. Geophys. Res., 68, 2559-2570, 1963.

Rishbeth, H., T. E. VanZandt, and R. B. Norton, "Diffusive Equilibrium in the Topside Equatorial Ionosphere," Annales Geophys., 22, 538-548, 1966.

Sato, T., "Electron Density Variations in the Topside Ionosphere Between 60° N and 60° S Geomagnetic Latitude Associated with Geomagnetic Disturbances," J. Geophys. Res., 73, 6225-6241, 1968.

Spreiter, John R., and Benjamin R. Briggs, "Theory of Electrostatic Fields in the Ionosphere at Equatorial Latitudes," J. Geophys. Res., 66, 2345-2354, 1961.

Thomas, J. O., "The Electron Density Distribution in the F Region of the Ionosphere" in Electron Density Profiles, ed. by B. Maehlum, Pergamon Press (1962).

Thomas, L., "The F2 Region Equatorial Anomaly During Solstice Periods at Sunspot Maximum," J. Atmos. Terr. Phys., 30, 1631-1640, 1968.

Varnasavang, V., "Nighttime F2 Layer at the Equator," J. Geophys. Res., 72, 1555-1561, 1967.

Varnasavang, V., Sylvia Hargreaves, and P. C. Kendall, "The Influence of Horizontal Air Motions on F2 Region Ionization," J. Atmos. Terr. Phys., 27, 707-721, 1965.

Windle, D. W. and P. C. Kendall, "A Possible Explanation of the Appleton Anomaly of the F2 Layer II. A Model with Unequal Horizontal Velocities," J. Atmos. Terr. Phys., 27, 1163-1168, 1965.

FIGURE CAPTIONS

Figure 1. Constant height profiles of electron density with magnetic dip averaged for noon for September, 1957; average peak electron density $N_m F2$ is also shown. The zero of the scale for each height is marked. (After Croom, Robbins, and Thomas, 1959).

Figure 2. Comparison of theoretical curves with Alouette observations over Singapore as provided by J. W. King. (After Goldberg, Kendall, and Schmerling, 1964).

Figure 3. Theoretical behavior of $N_m F2$ and $h_m F2$ with dip latitude under conditions of variable electron temperature. (After Goldberg, 1965.)

Figure 4. A vector plot of theoretical electron fluxes for conditions of sunspot maximum and an upward electrodynamic drift of 10 m/s. Magnetic field lines are shown every 200 km. (After Hanson and Moffett, 1966.)

Figure 5. Theoretical contours of electron density as a function of dip latitude and height for an upward drift of 20.5 m/s. The contour units are 10^5 el. cm^{-3}. The dashed curve represents a magnetic field line. The dotted curve is the locus of points of the geomagnetic anomaly crests. (After Bramley and Peart, 1965.)

Figure 6. Theoretical distribution of electrons that is asymmetrical about the equator owing to a north-south wind in the neutral atmosphere of 60 m/s, conditions of sunspot maximum, and an upward drift of 15 m/s. The values of h_mF2 are given for several different dip latitudes along the N_mF2 curves. (After Hanson and Moffett, 1966.)

Figure 7. Theoretical world curves of N_mF2 for an upward drift of 20 m/s under conditions approximating sunspot maximum. The contour numbers are proportional to an arbitrary maximum electron production rate. For $q_0 = 1625\ \mathrm{cm}^{-3}\ \mathrm{sec}^{-1}$, the scaling factor would be 6×10^5 el. cm^{-3}. (After Baxter and Kendall, 1968.)

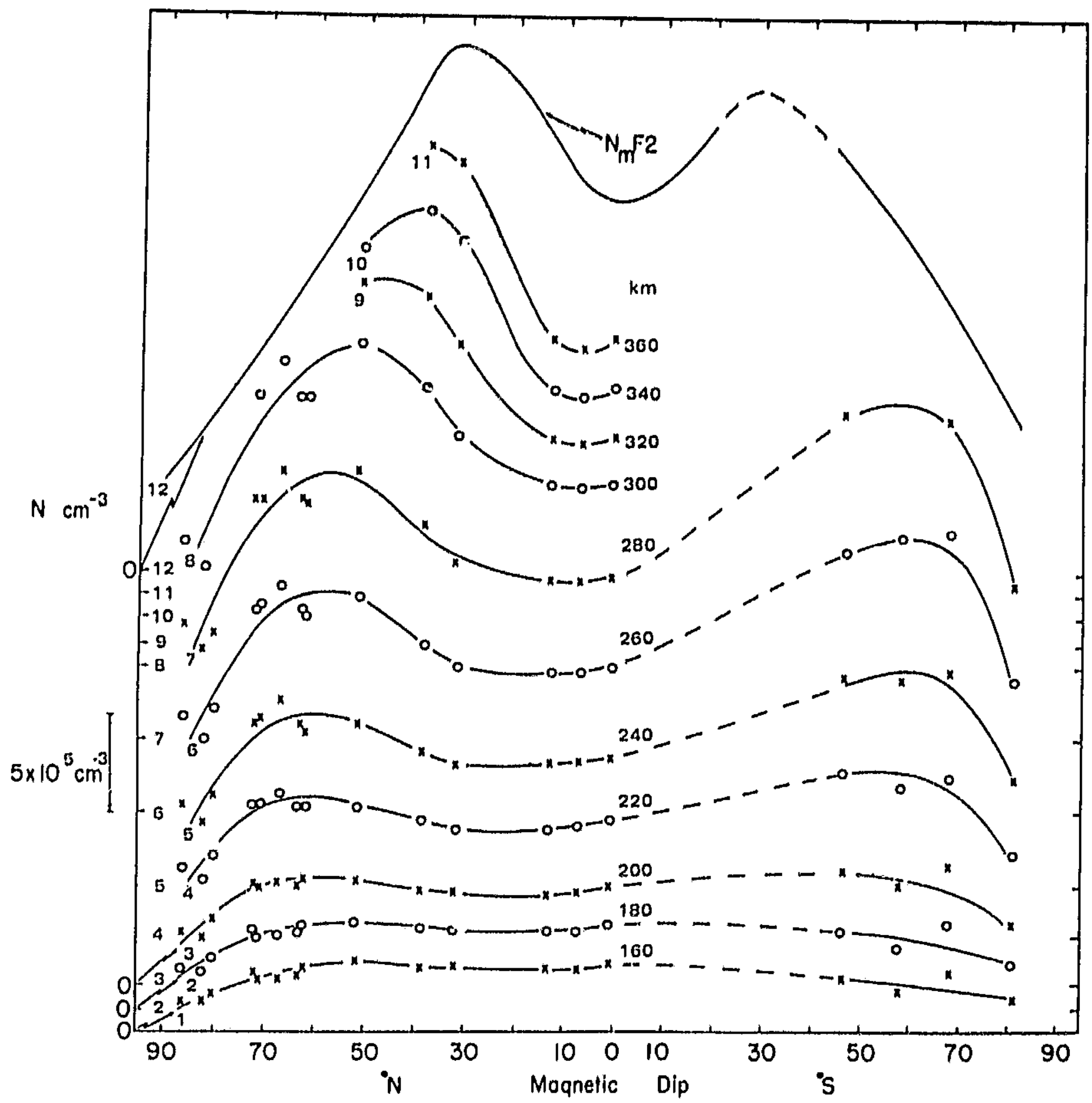

N_mF2
km
360
340
320
300
280
260
240
220
200
180
160
N cm^{-3}
5×10^5 cm^{-3}
90
70
50
30
10
0
10
30
50
70
90
°N
Magnetic Dip
°S

Figure 1

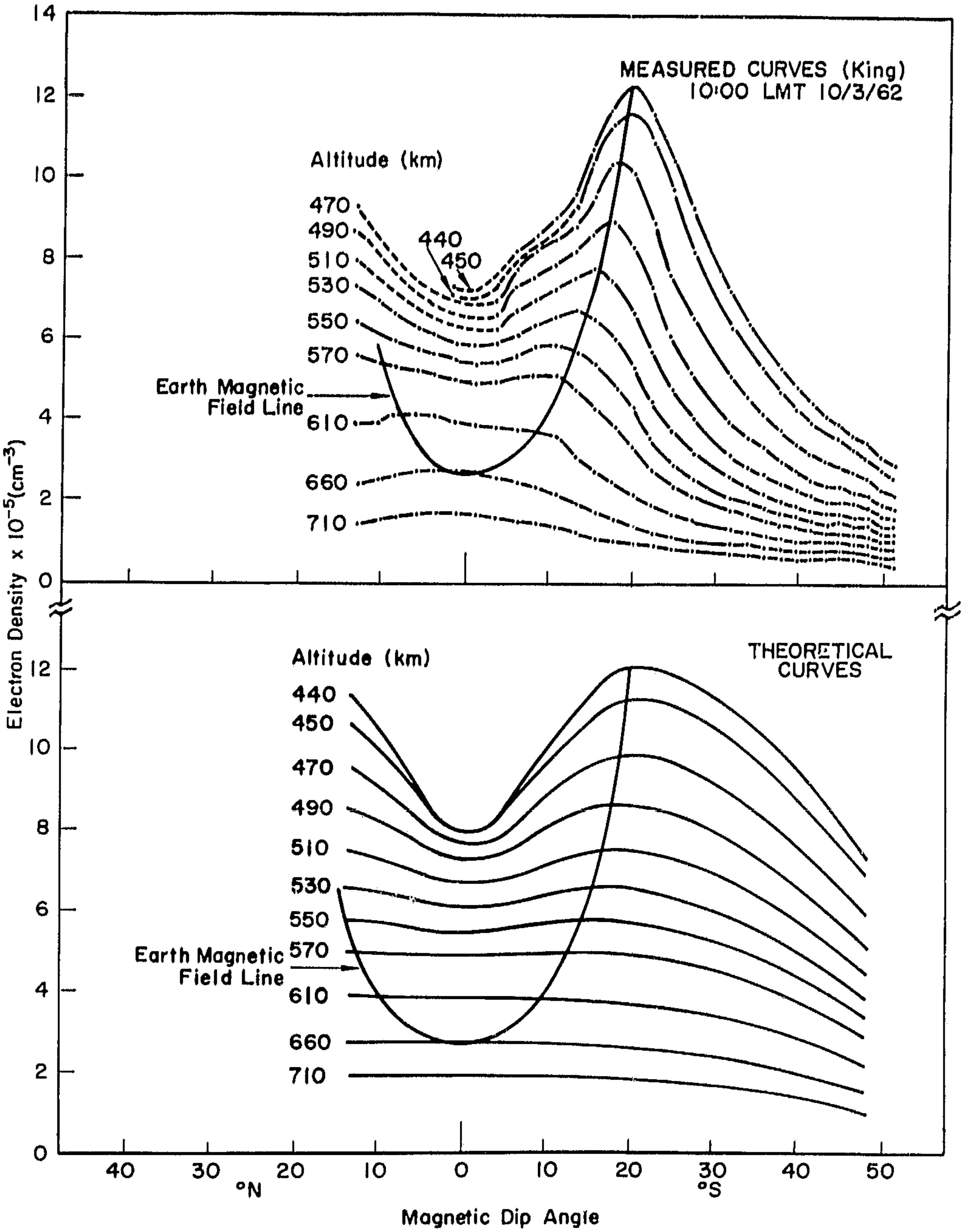
MEASURED CURVES (King)
10:00 LMT 10/3/62
Altitude (km)
470
490
510
530
550
570
610
660
710
440
450
Earth Magnetic Field Line
THEORETICAL CURVES
Altitude (km)
440
450
470
490
510
530
550
570
610
660
710
Earth Magnetic Field Line
Electron Density x 10^{-5}(cm^{-3})
14
12
10
8
6
4
2
0
40
30
20
10
0
10
20
30
40
50
°N
°S
Magnetic Dip Angle

Figure 2

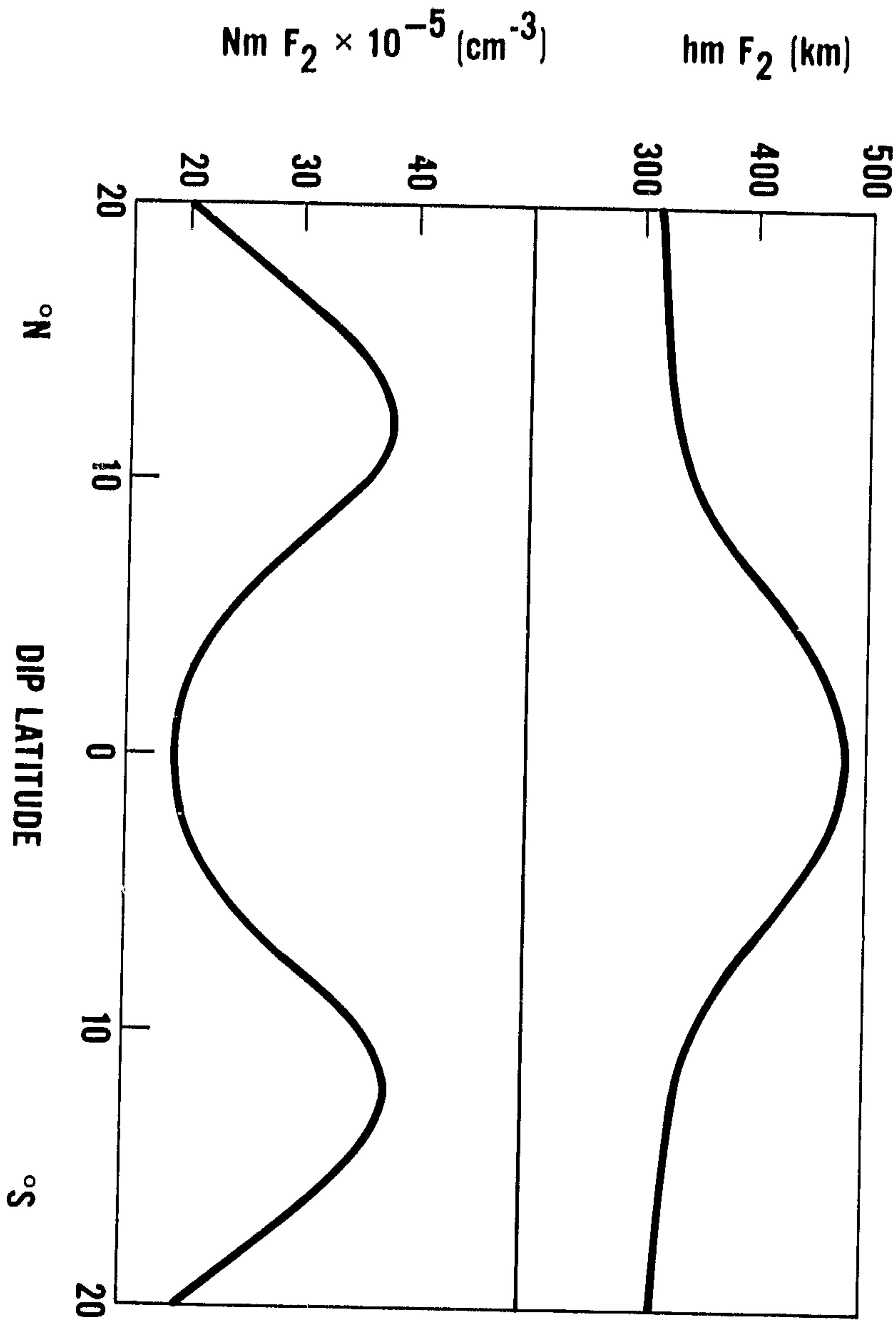

hm F2 (km)
500
400
300
Nm F2 × 10^−5 (cm^-3)
40
30
20
°N
20
10
0
10
20
°S
DIP LATITUDE

Figure 3

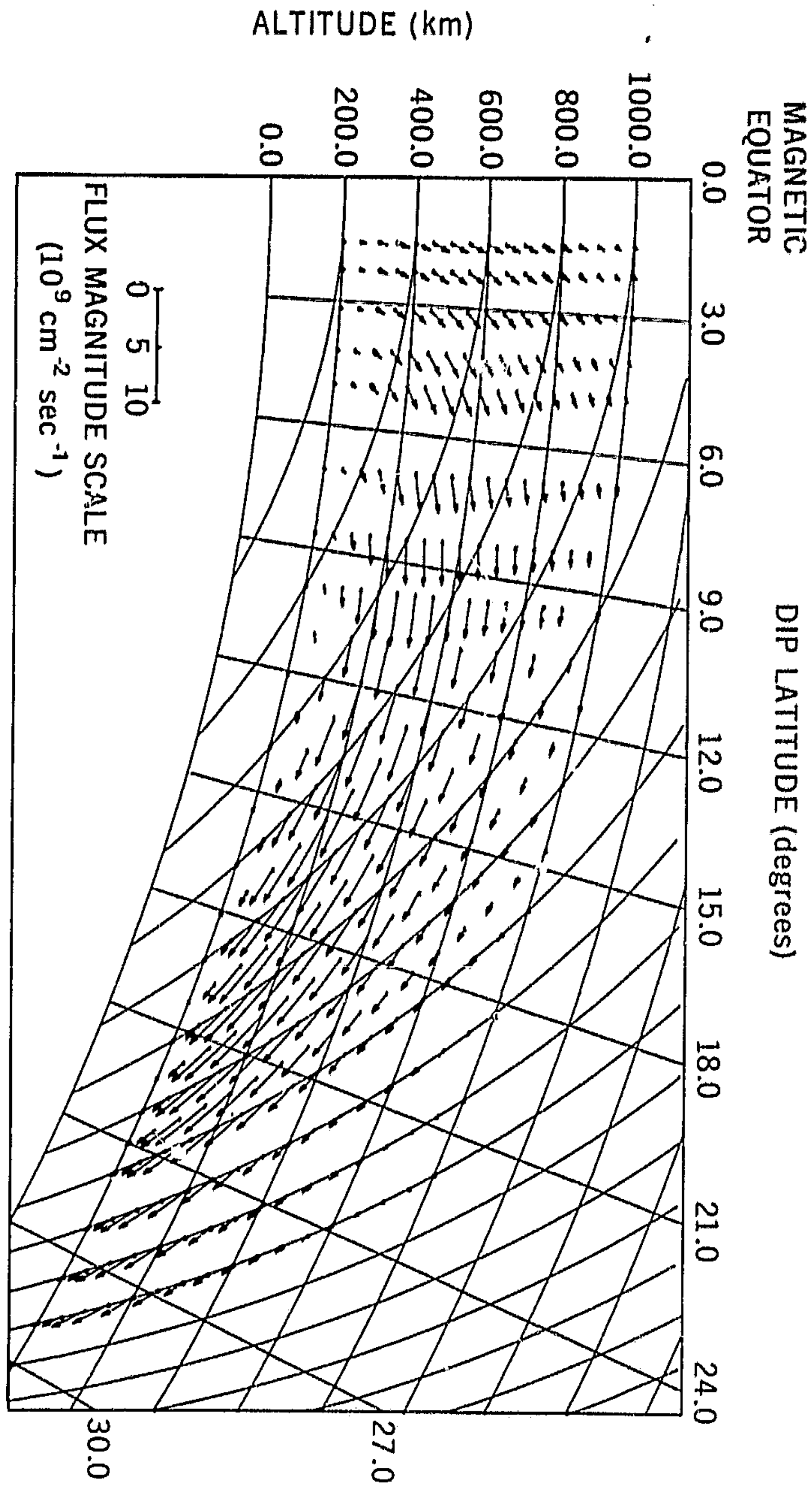

ALTITUDE (km)
MAGNETIC EQUATOR
1000.0
800.0
600.0
400.0
200.0
0.0
0.0
3.0
6.0
9.0
12.0
15.0
18.0
21.0
24.0
27.0
30.0
DIP LATITUDE (degrees)
0 5 10
FLUX MAGNITUDE SCALE
(10^9 cm^{-2} sec^{-1})

Figure 4

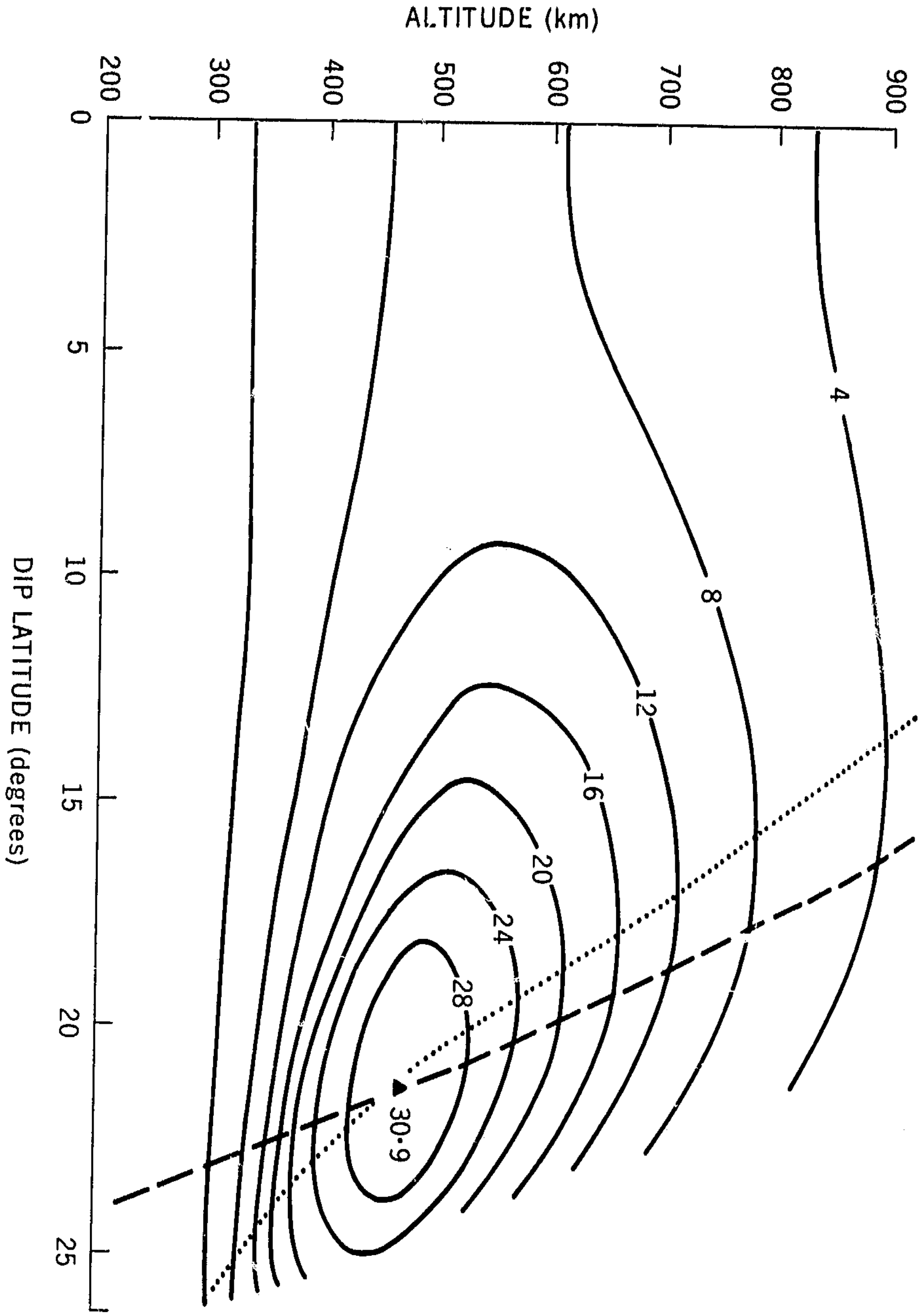
ALTITUDE (km)
200
300
400
500
600
700
800
900
0
5
10
15
20
25
DIP LATITUDE (degrees)
4
8
12
16
20
24
28
30·9

Figure 5

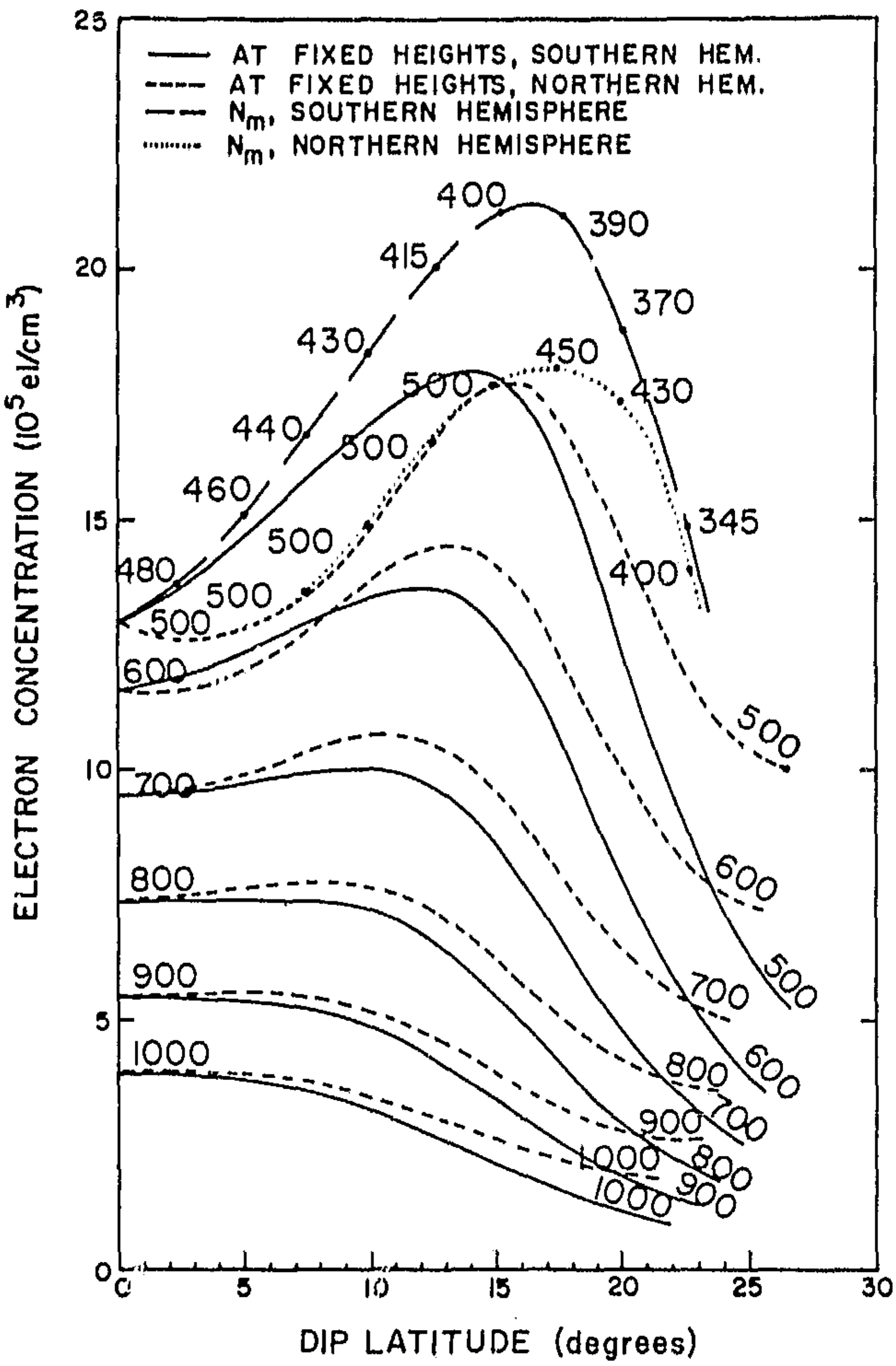

AT FIXED HEIGHTS, SOUTHERN HEM.
AT FIXED HEIGHTS, NORTHERN HEM.
Nm, SOUTHERN HEMISPHERE
Nm, NORTHERN HEMISPHERE
400
390
415
370
430
450
500
430
440
500
460
345
500
400
480
500
500
600
500
700
600
800
500
700
900
800
600
1000
900
700
1000
800
900
1000
ELECTRON CONCENTRATION (10^5 el/cm^3)
DIP LATITUDE (degrees)

Figure 6

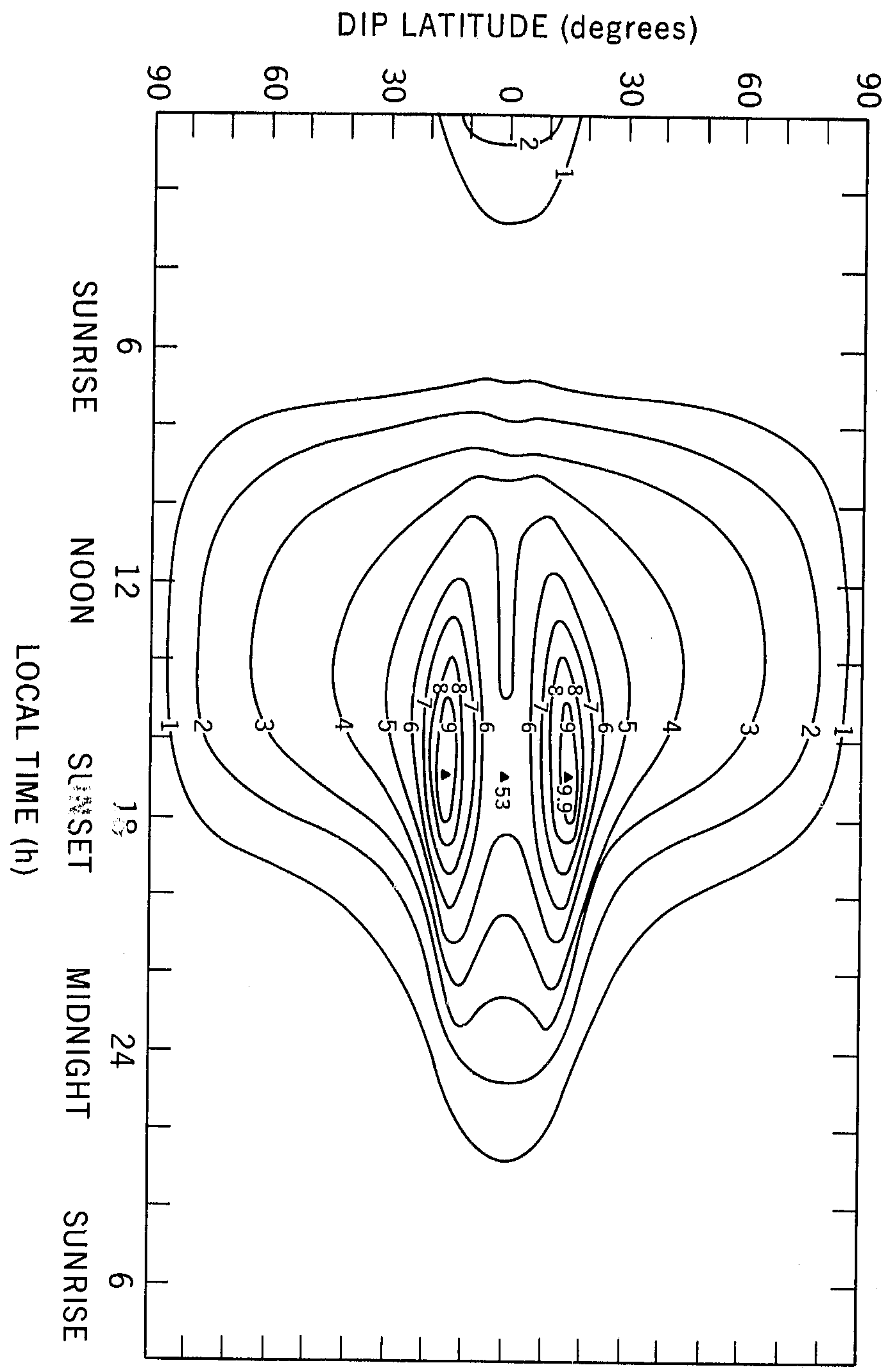
DIP LATITUDE (degrees)
90
60
30
0
30
60
90
6
SUNRISE
12
NOON
18
SUNSET
24
MIDNIGHT
6
SUNRISE
LOCAL TIME (h)
1
2
3
4
5
6
7
8
9
9.9
53

Figure 7